NRL REPORT 3707

FR-3707

TRANSIENT ELECTRICAL CHARACTERISTICS OF LEAD-ACID SUBMARINE BATTERIES

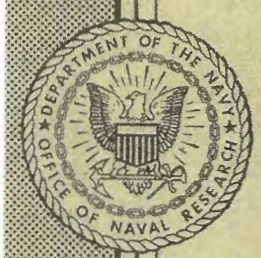

NAVAL RESEARCH LABORATORY

WASHINGTON, D.C.

NRL REPORT 3707

TRANSIENT ELECTRICAL CHARACTERISTICS OF LEAD-ACID SUBMARINE BATTERIES

B. G. Bingham

June 30, 1950

Approved by:

Mr. A. T. McClinton, Head, Shipboard Systems Branch
Dr. W. C. Hall, Superintendent, Electricity Division

NAVAL RESEARCH LABORATORY
CAPTAIN F. R. FURTH, USN, DIRECTOR
WASHINGTON, D.C.

DISTRIBUTION

CNO	1
BuShips	
Attn: Code 660	1
Attn: Code 660U	10
CO, USNSB, New London	1
BuAer	
Attn: Code Aer-EL-61	3
CO and Dir., USNEL	2
CDR, USNOTS	
Attn: Reports Unit	2
OCSigO	
Attn: Ch. Eng. & Tech. Div., SIGTM-S	1
CO, SCEL	
Attn: Dir. of Eng.	2
Wright-Patterson AFB	
Attn: BAU-CADO	1
Attn: CADO-E1	2
Div. of Public Documents, G. P. O.	
Attn: Library	1
RDB	
Attn: Information Requirements Branch	2
Attn: Navy Secretary	1
Naval Res. Sec., Science Div., Library of Congress	
Attn: Mr. J. H. Heald	2

CONTENTS

Abstract	iv
Problem Status	iv
Authorization	iv
INTRODUCTION	1
INTERNAL RESISTANCE CHARACTERISTICS	3
OVERVOLTAGE PHENOMENA	8
MAXIMUM FAULT CURRENTS	9
RECOVERY VOLTAGE	10
CONCLUSIONS	12
RECOMMENDATIONS	13
ACKNOWLEDGMENTS	13
APPENDIX I - Experimental Results on the Guppy Cell (Type MAQ-71)	14
APPENDIX II - Experimental Results on the Sargo Cell (Type VLA-47)	21

ABSTRACT

The transient characteristics of submarine cells have been studied to determine the importance and order of magnitudes of such factors as effective internal resistance, internal voltage, and recovery voltage. These factors have been determined quantitatively for various operating conditions and for step loads up to short circuit on the battery.

The results reveal the importance of overvoltage which exists during charging and the contribution it makes to short-circuit currents. However, the overvoltage was found to contribute very little to the magnitude of recovery voltage after short circuit. Data is also presented to show the variation of internal resistance for all battery conditions. Recommendations are made for values of internal resistance and voltage to be used in system analysis work.

PROBLEM STATUS

This is a final report on this phase of the project. Work on the problem is continuing.

AUTHORIZATION

NRL Problem E01-05R

(BuShips ltr. SS/60 (660U-330) dated 26 September 1947.)

NS 676-003

TRANSIENT ELECTRICAL CHARACTERISTICS OF LEAD-ACID SUBMARINE BATTERIES

INTRODUCTION

In the past the rather uncritical requirements for circuit breakers and other protective devices made it unnecessary for the designer to take the battery behavior into very strict account. The coordination and specification of operating and protective breakers concerned with the submarine battery have previously been obtained by assuming that static and transient battery characteristics were identical. In other words, the battery could be considered a passive constant-voltage source in the system.

The new submarines with their higher capacity batteries, generators, and motors emphasize the need for accurate information in determining breaker interrupting capacity while maintaining minimum size and weight. Such information can be obtained only by examining the action of all system components for various machinery combinations and operating conditions.

During the study of the short-circuit characteristics of a mock submarine it was observed that the behavior of the battery departed sufficiently from the passive

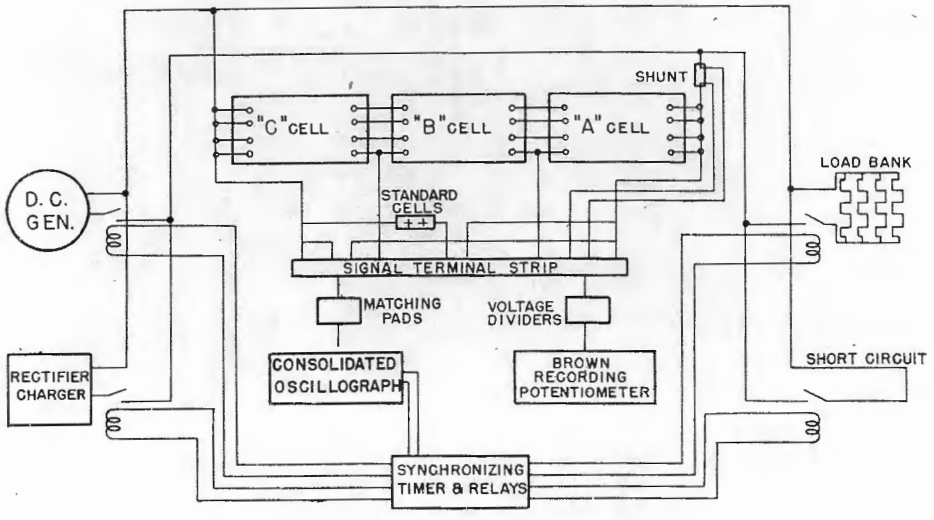

Figure 1 - Schematic diagram of battery power, control and instrumentation circuit. Laboratory tests on Guppy cell (Type MAQ-71).

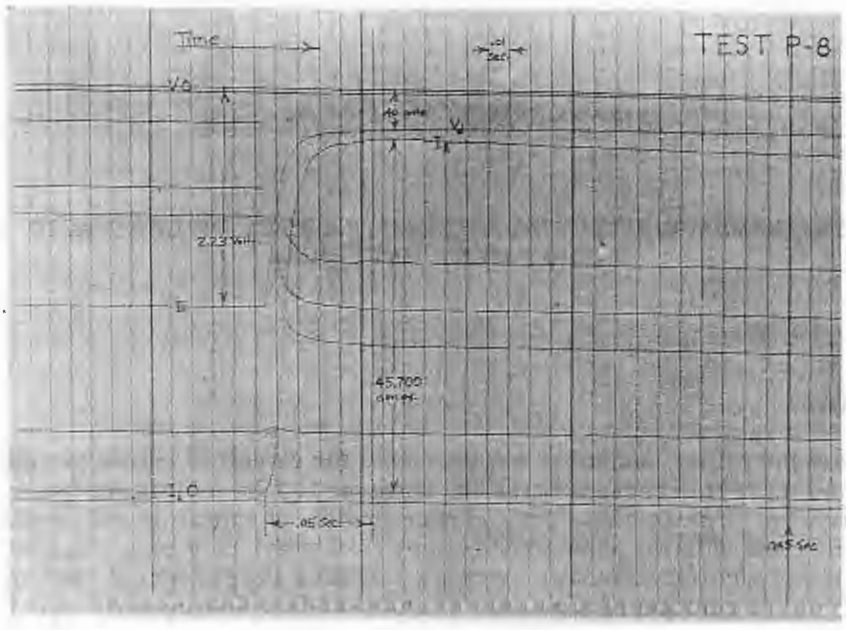

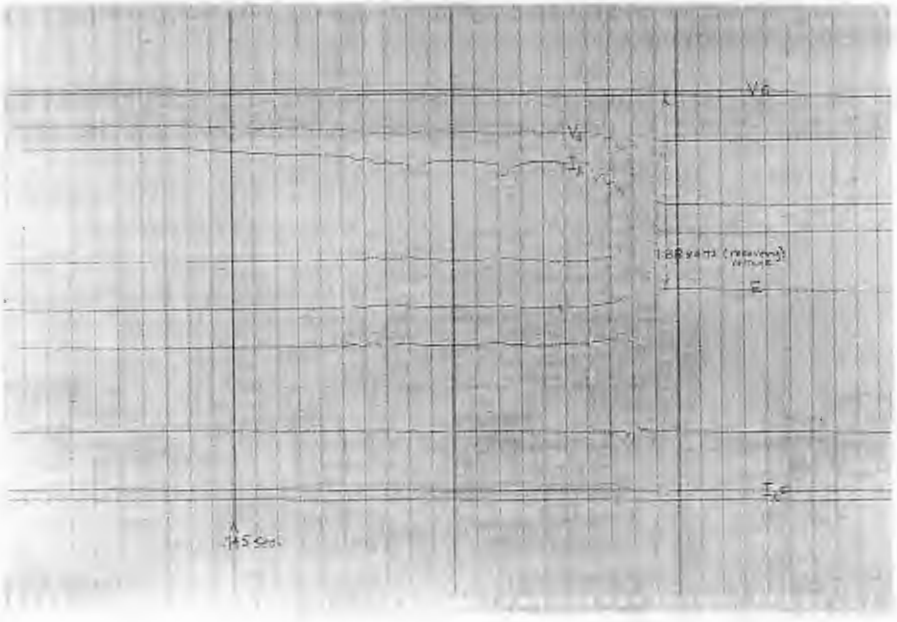

Figure 2 - Typical oscillograms from Guppy cell tests
- V_o - Zero position of voltage trace
- I_{1o} - Zero position of current trace
- E - Battery internal voltage
- V_d - Battery terminal voltage during loading
- I_1 - Battery load current

constant-voltage assumption to affect seriously the accuracy of calculation resulting from these previous methods. An investigation was therefore undertaken to determine the variations in the internal resistance and voltage of the battery with operating conditions and to determine their effect on the calculations of fault currents in a system. Specifically, the facts sought were (a) dependence of the internal resistance on load, (b) variation of overvoltage and its power capacity, and (c) dependence of the recovery voltage at the battery terminals on load and time.

The schematic diagram of the laboratory test set-up employed to obtain this information is shown in Figure 1. The battery current and terminal voltage were obtained from oscillograms and then used for computing other data. Figure 2 is an example of the oscillograms. The schematic diagram of the generator-battery system is shown in Figure 3. The instrumentation and automatic control were essentially the same as that employed in Figure 1. Figure 4 is a typical set of oscillograms obtained from these system studies. All details of the various test conditions, data interpretation, and calculations are given in Appendices I and II.

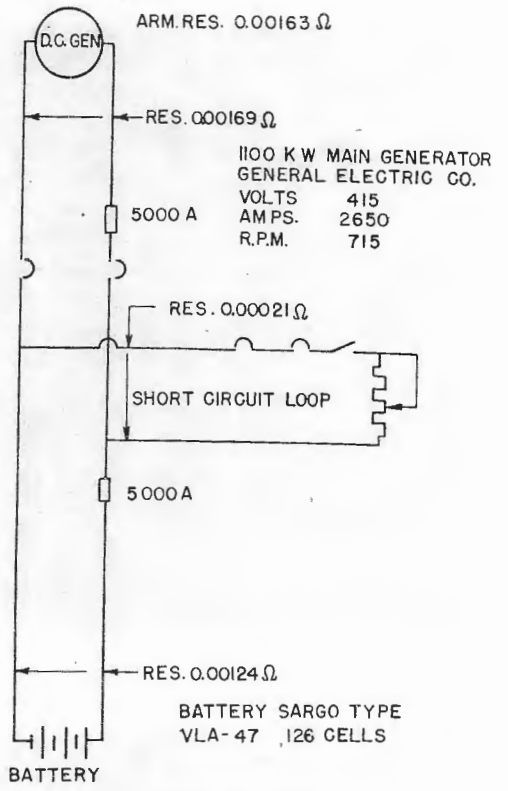

Figure 3 - Schematic diagram of generator-battery circuit. Systems tests on Sargo cell (Type VLA-47).

INTERNAL RESISTANCE CHARACTERISTICS

The battery internal resistance varied significantly during the charging cycle and with load, as evidenced by the curves of Figure 5 for the Guppy cell and Figure 6 for the Sargo cell.

The high initial resistance of the cells in the discharged condition is due largely to the low specific gravity and resulting low conductivity of the electrolyte. As the battery is charged, the resistance decreases because of increasing specific gravity. The negative coefficient of resistivity of the electolyte with rising temperature also results in a decreasing resistance. When the battery EMF increases past its nominal value and overvoltage appears, the value of effective internal resistance begins to rise. This increase is particularly evident at the lower loads because the lower the load the larger is the percentage of IR drop due to overvoltage. The increasingly heavy gassing present during the latter portion of the charge also tends to raise the resistance. The region "A" in Figures 5 and 6 represents the battery floating on the charging line, taking no charging current. The resistance decreases rapidly in this region because there is practically no overvoltage present and hence no component of effective resistance due to overvoltage destruction.

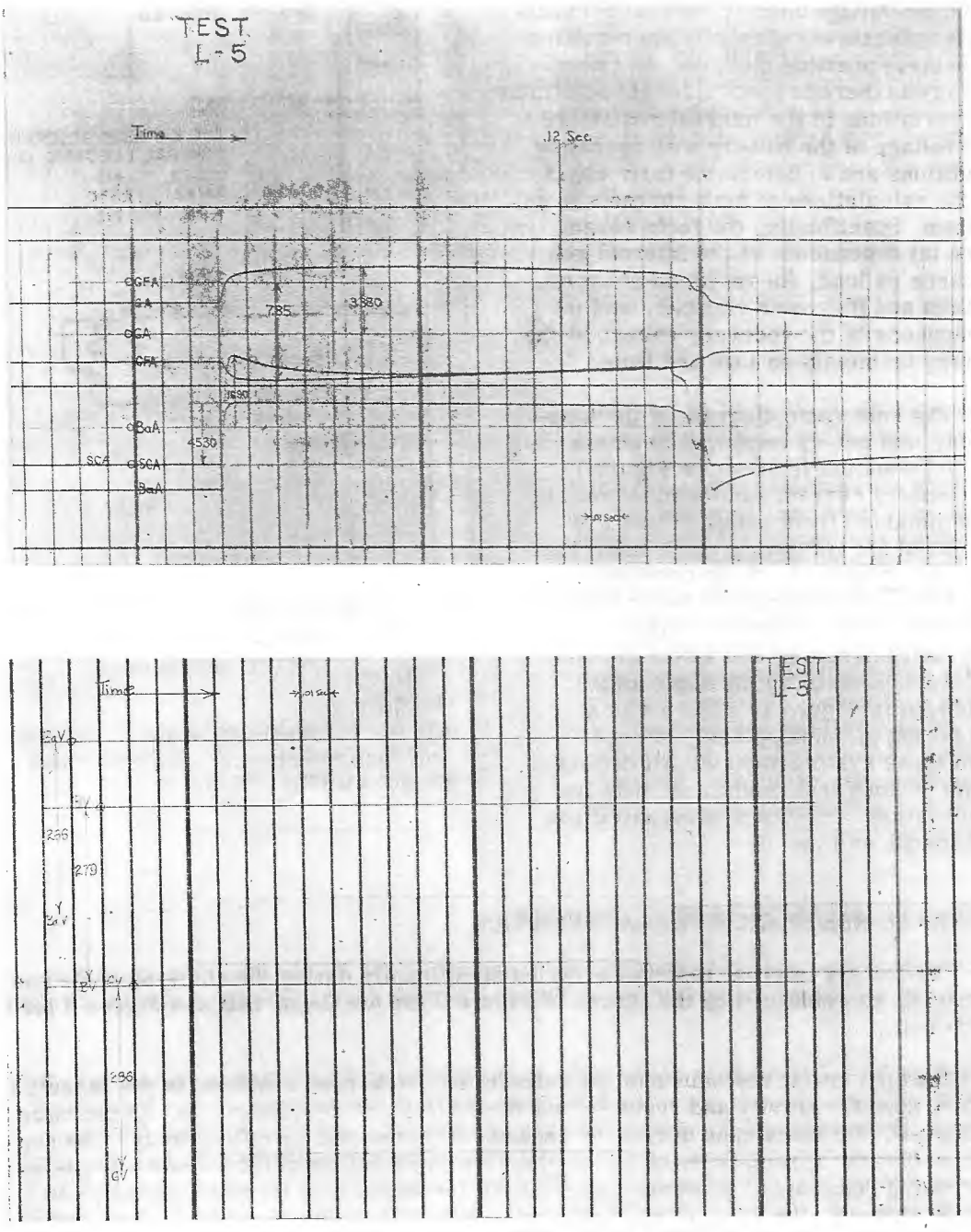

Figure 4 - Typical oscillograms for Sargo cell tests
GA - Generator armature current
GFA - Generator field current
BaA - Battery current
SCA - Short-circuit current (generator + battery)
GV - Generator terminal voltage
BaV - Battery terminal voltage
BV - Bus voltage
O - Indicates zero position of trace

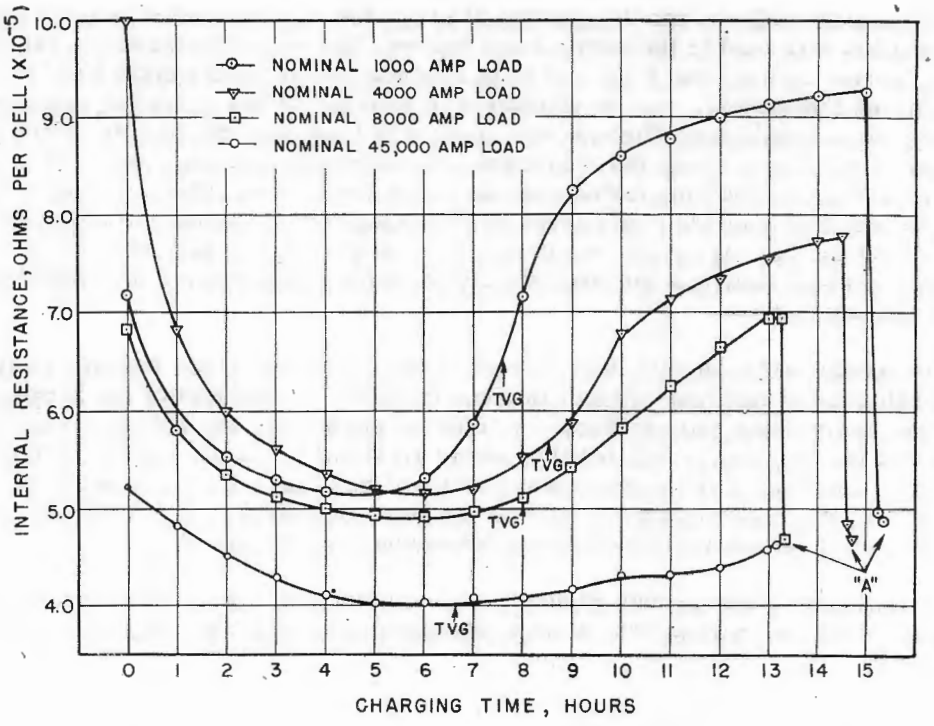

Figure 5 - Effective internal resistance of the Guppy cell (MAQ-71) during the charging cycle

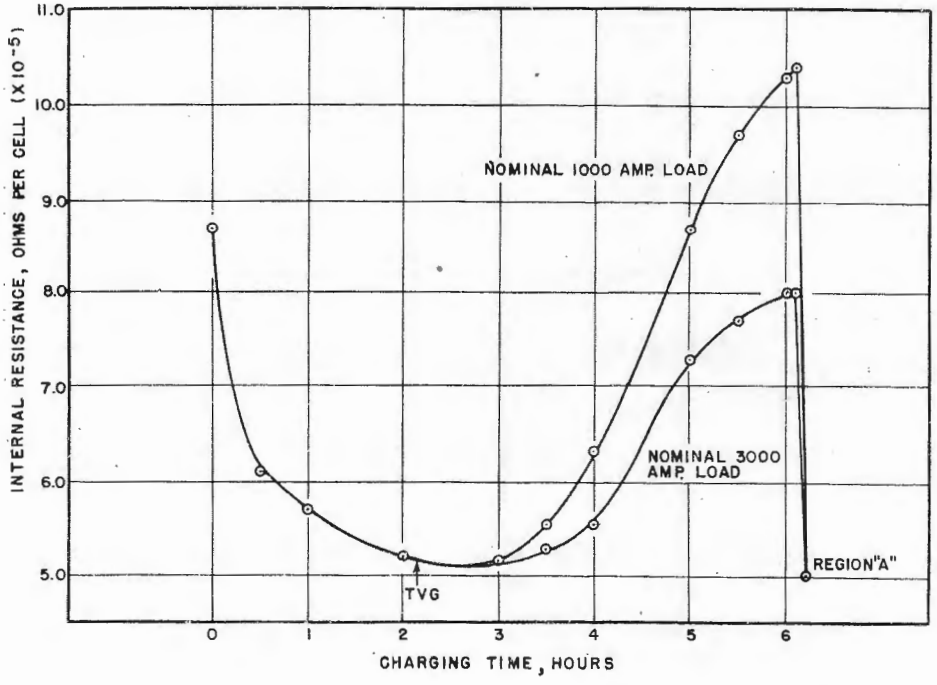

Figure 6 - Effective internal resistance of the Sargo cell (VLA-47) during the charging cycle

This explanation suffices for the general shape of the internal resistance curves and the wide variation with load in the overvoltage region. The smaller resistance variation with load, apparent up until the TVG[1] curve is reached (and probably underlying the larger variations thereafter), may be attributed to a factor called "transfer resistance." This quantity has a negative coefficient with respect to load current, and its effect is enhanced by gassing. There are in the literature several conflicting theories as to the cause of this factor, and nothing further can be conjectured here. The crossing of the 1000-ampere and 4000-ampere load curves is not considered to represent a significant characteristic of the battery. It is considered that a slight shift in the zero charge condition of the cells has occurred and that this circumstance accounts for the apparent crossing of the two curves.

The resistance variation with load current of the Guppy cell (fully charged on finishing rate and floating at nominal voltage) is given in Figure 7, and that of the Sargo cell (fully charged on finishing rate) in Figure 8. Similar curves for any battery condition could be drawn for the Guppy cell, but they would all lie in the range defined by the two curves shown. A further point of importance that will be observed from comparing Figures 5 and 6, and Figures 7 and 8, is that the general shape of the curves and the range of resistance values are the same for both Guppy and Sargo cells.

All the characteristics through Figure 8 were obtained during a charging cycle and include the effect of the two factors, state of charge and overvoltage. In order to

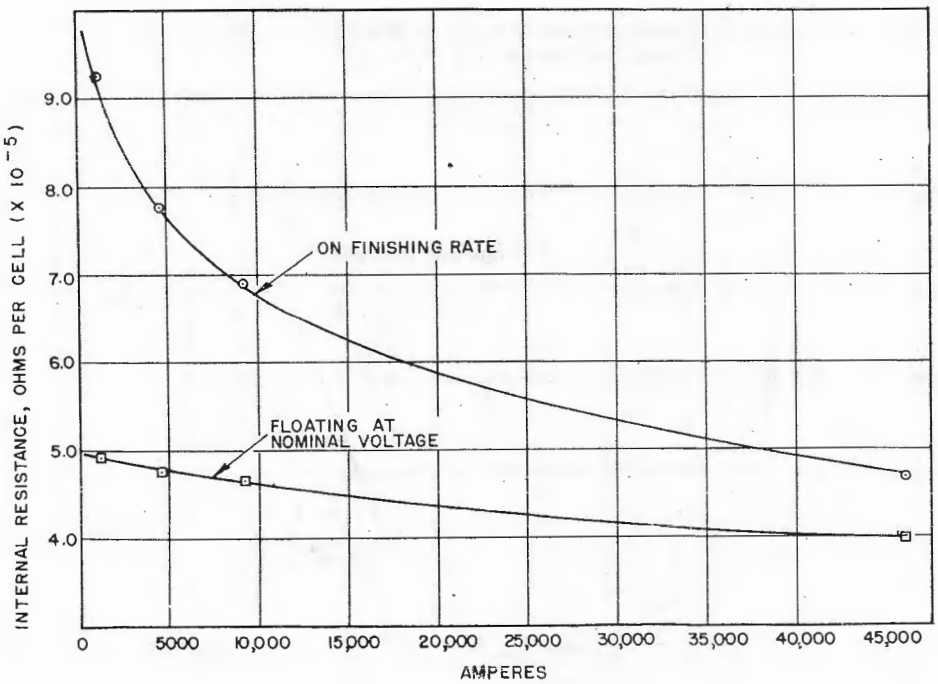

Figure 7 - Effective internal resistance of the fully charged Guppy cell (MAQ-71)

[1]Temperature-Voltage-Gassing curve: A theoretical curve which specifies the values of temperature and voltage at which gassing will begin during the charging cycle.

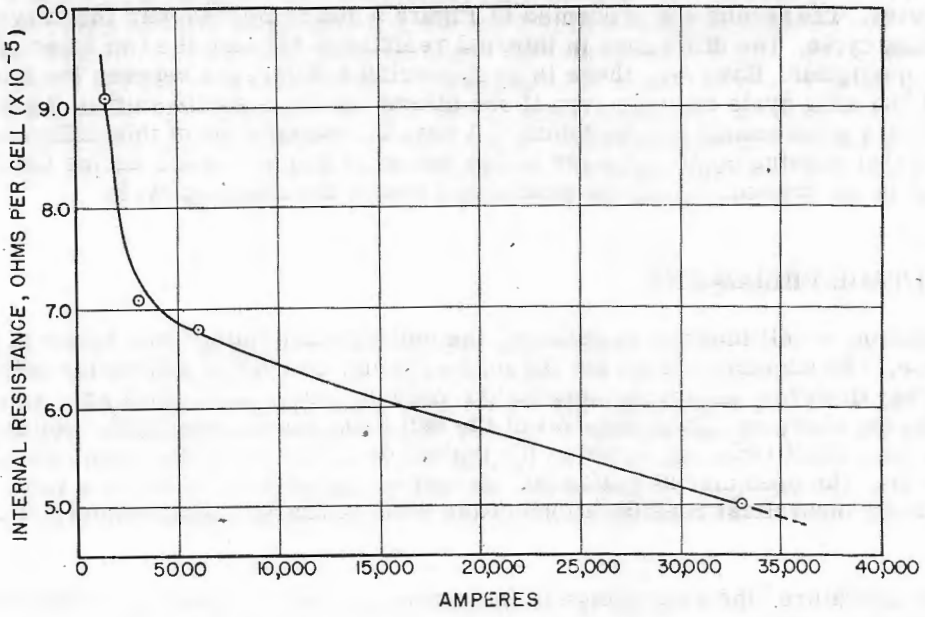

Figure 8 - Effective internal resistance of the fully charged Sargo cell (VLA-47) on finishing rate

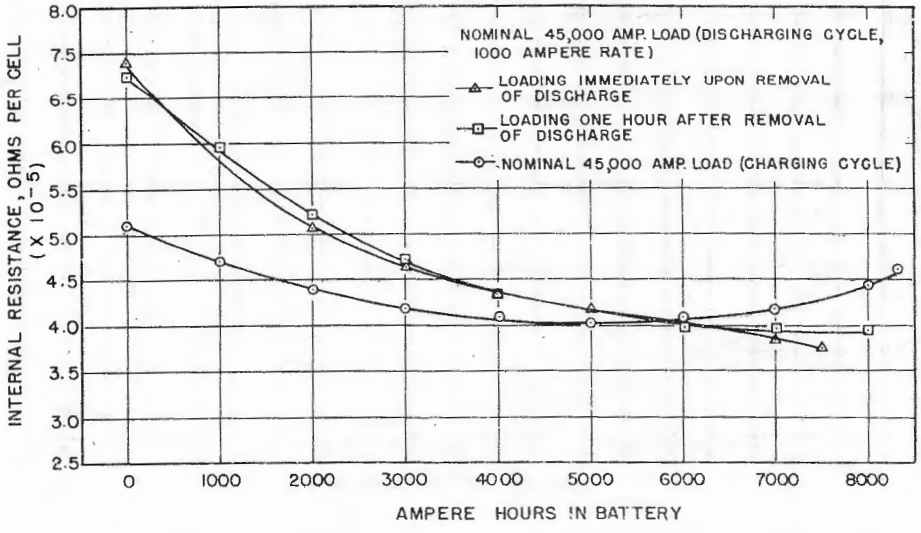

Figure 9 - Effective internal resistance of the Guppy cell (MAQ-71) for maximum loads during charge and discharge cycles

eliminate the effect of overvoltage, the internal resistance was obtained during two discharge cycles. The results are presented in Figure 9 and compared with the curve from the charging cycle. The difference in internal resistance between the two types of discharge is negligible. However, there is an appreciable difference between the discharge cycle and charging cycle curves, even if one allows for the possible shift in the zero-ampere-hours point mentioned previously. A possible explanation of this difference lies in the fact that gassing continues down to low values of ampere-hours during the discharge but is not present during the similar portion of the charging cycle.

OVERVOLTAGE PHENOMENA

In addition to cell internal resistance, the cell internal voltage is a factor of major importance. The nominal voltage for the lead-acid cell as used in submarine batteries is 2.1 volts. However, an appreciably higher voltage, known as overvoltage, exists in the cell during charging. Upon removal of the cell from charge this higher voltage will disappear in a short time, as shown in the typical decay curve of the Sargo cell plotted in Figure 10. The open circuit voltage of the cell will gradually reduce to a value determinable by theoretical considerations of the state of charge, temperature, etc., of the cell.

In the literature[2] the overvoltage is interpreted as due to a local concentration of the electrolyte in the pores and near the surface of the battery plates during charging; but no theoretical basis for calculating its value has appeared. It is known to exist throughout the charging cycle but does not cause the cell internal voltage to rise above the nominal 2.1 volts until the battery is, in terms of ampere-hours, about one-quarter to one-half charged. The way in which the overvoltage appears during the charge is shown in Figure 11 (on the internal voltage curve of the Sargo cell) and in Figure 12 (on a typical recorded voltage curve of the Guppy cell).

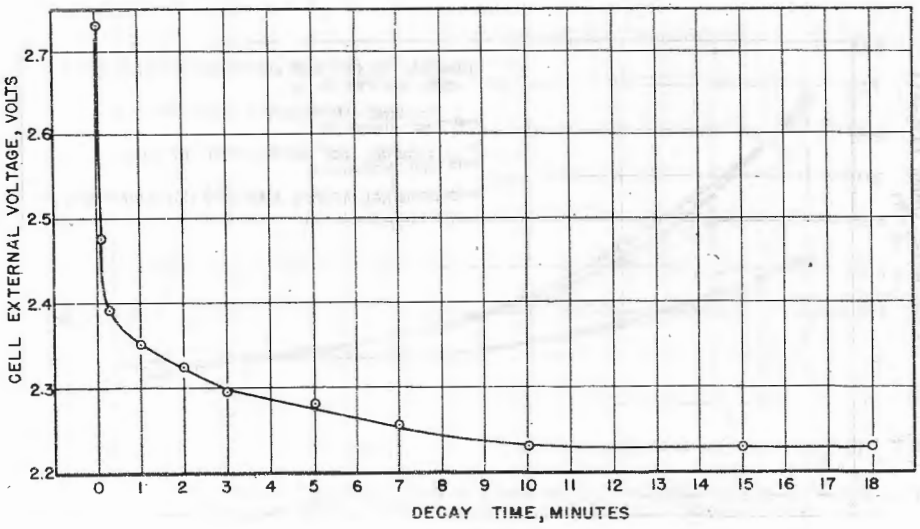

Figure 10 - Internal voltage decay curve of fully charged Sargo cell (VLA-47) on removal from charge

[2]Vinal, G. W., "Storage Batteries," Third Edition, J. Wiley & Sons, New York, 1940

Of greater importance than the existence of this overvoltage is its ability to supply current to transient loads, as illustrated by Figure 13. It is to be noted that the current recorded immediately after application of a step load is a function of the battery voltage at the instant of loading. One must therefore look upon the overvoltage as a real voltage capable of furnishing at least a transient current. The high cell voltages shown in Figure 13 were obtained by putting a fully charged battery at a temperature of 85° F at the finishing rate.

MAXIMUM FAULT CURRENTS

The maximum fault current obtained during these battery studies was limited by two factors: The cell effective internal resistance and the external circuit resistance. Experimental evidence of fault current with zero external resistance is impossible; therefore, the maximum

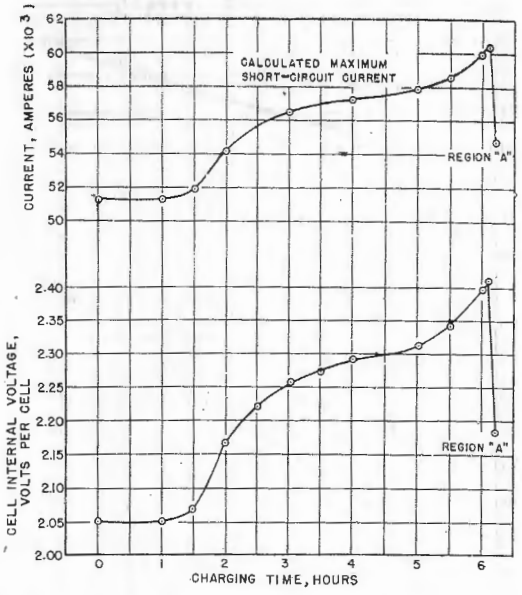

Figure 11 - Battery internal voltage and calculated maximum short-circuit current of the Sargo cell (VLA-47) during the charging cycle

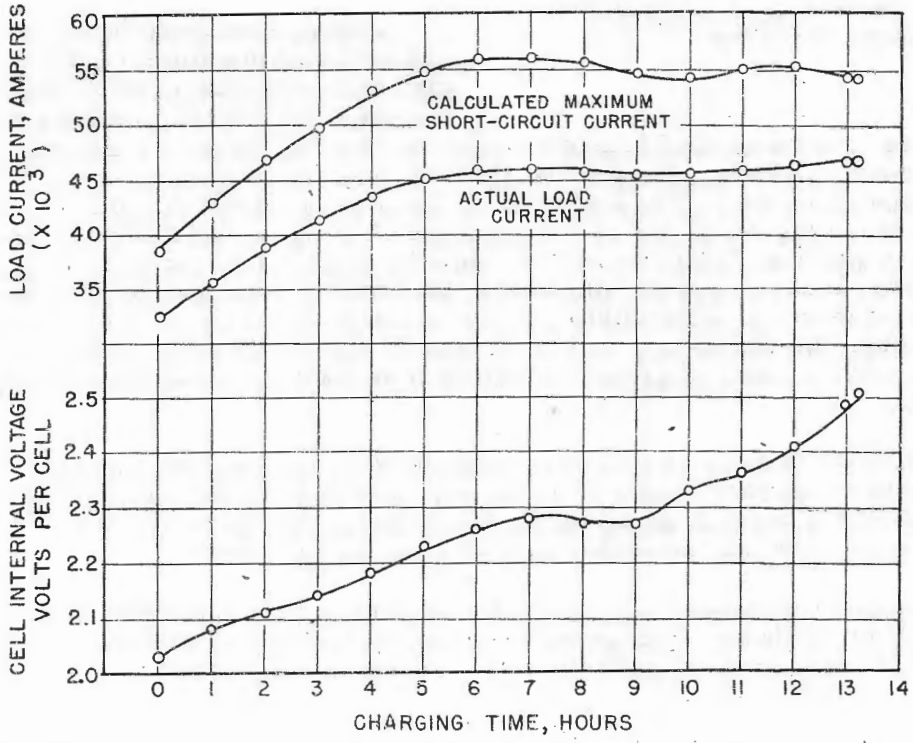

Figure 12 - Battery internal voltage and calculated maximum short-circuit current of the Guppy cell (MAQ-71) during the charging cycle

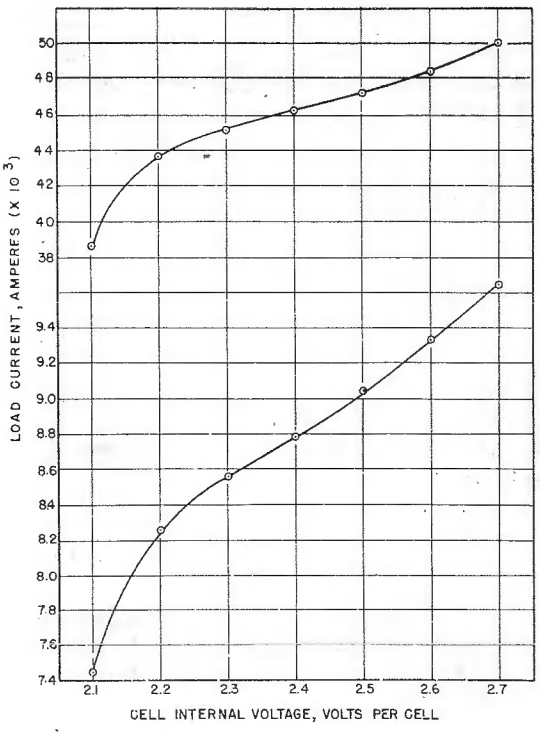

Figure 13 - Overvoltage capacity of the Guppy cell (MAQ-71)

current had to be obtained by computation. In making this computation for the Sargo cell the curve (internal resistance versus load current) of Figure 8 was extended to 45,000 amperes. The result is a value of approximately 40 micro-ohms, which was used in conjunction with the cell-voltage curve in Figure 11 to calculate the maximum short-circuit current curve (also shown in Figure 11). This curve is, of course, inaccurate to the extent that the variation of internal resistance throughout the charging cycle is not taken into account. The calculation of the maximum current for the Guppy cell is considerably more accurate because of the availability of internal resistance data in the 45,000-ampere range. Using this data and the typical cell-voltage curve in Figure 12, the maximum current curve was obtained. It is also plotted in Figure 12.

RECOVERY VOLTAGE

Although it was found that the overvoltage contained sufficient capacity to contribute to the value of short-circuit current, this voltage is in reality a transient in nature. After a few hundred ampere-seconds of loading, the battery internal voltage quickly recovers to a lower, stable value. Plots of these recovery voltages are shown in Figures 14 and 15 for the various load tests. It should be noted that all values of recovery voltage in Figures 14 and 15 were obtained after one second loading at the particular load in question. The 1000-, 4000-, and 8000-ampere-load curves show a trend --namely, lower recovery voltage with higher loads. However, considerable intermingling of the three curves results from variations in state of charge and in the value of cell voltage prior to loading. The 45,000-ampere load is found to depress the cell voltage below the nominal 2.1 volts, a condition probably resulting from depletion of electrolyte near the plate surfaces.

The difference in value of recovery voltage between charging and discharging cycles is probably due partly to a shift in the ampere-hour scale for the two tests. However, the absence of overvoltage during the discharge test and the temperature difference between the cells under the two conditions were contributing factors.

The relation between recovery voltage and transient loading expressed in ampere-seconds is shown in Figure 16. Although the initial voltage was not the same for all test points, the curve indicates the dependence of recovery voltage on load.

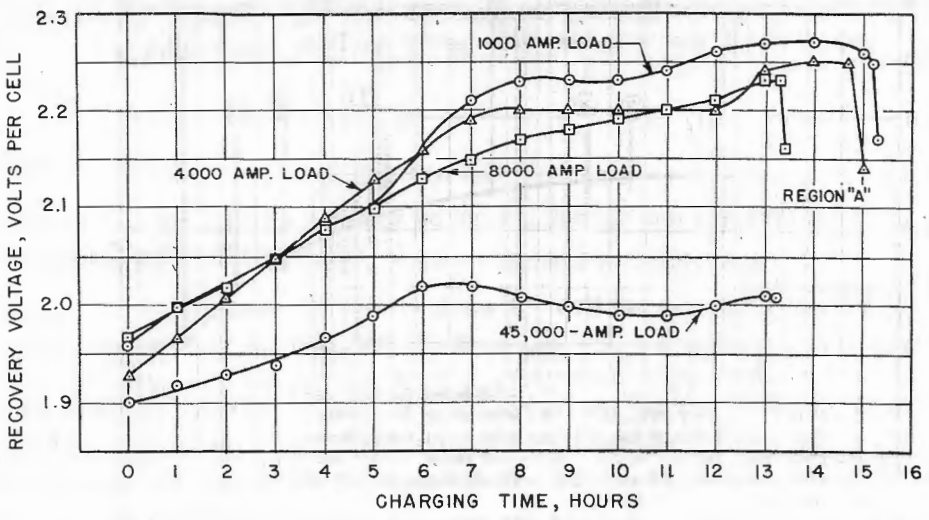

Figure 14 - Recovery voltage of the Guppy cell (MAQ-71) during the charging cycle

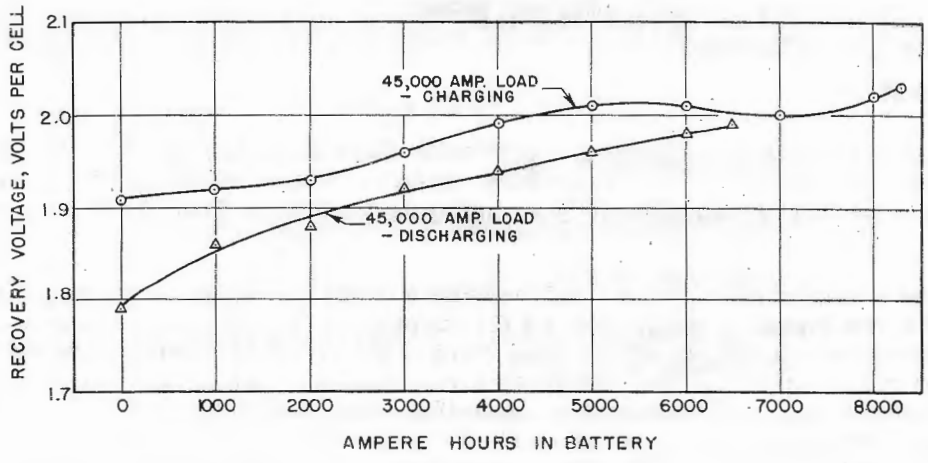

Figure 15 - Recovery voltage of the Guppy cell (MAQ-71) during the discharge cycle

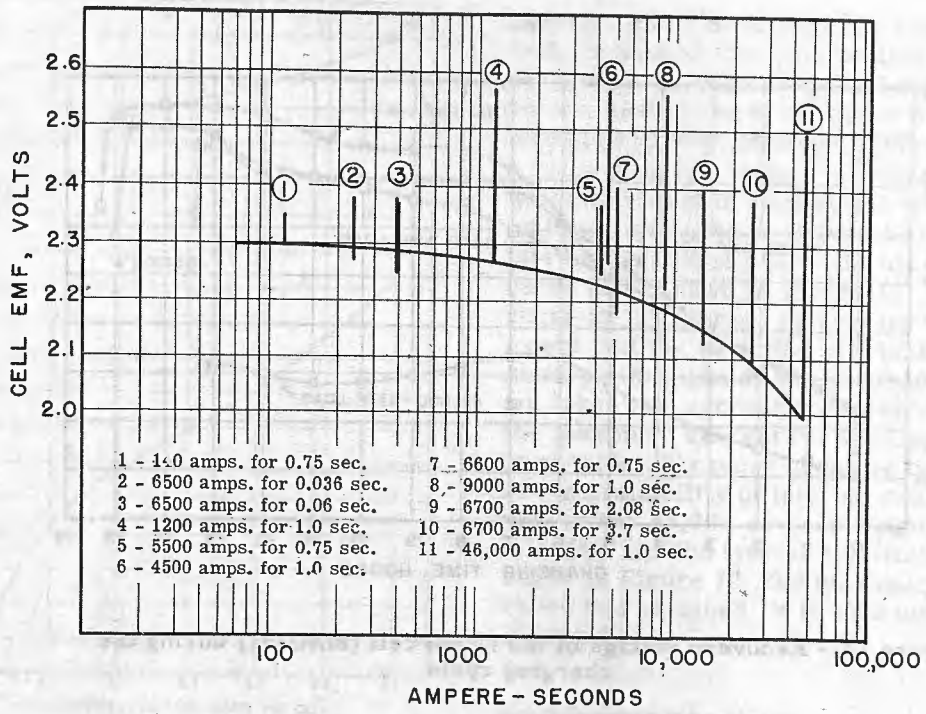

Figure 16 - Effect of load (ampere-seconds) on recovery voltage of Guppy cell (MAQ-71)

CONCLUSIONS

The results of this investigation, in particular those given in Figures 7, 9, 12, 13, and 16, show that battery internal resistance, internal voltage, short-circuit current, and recovery voltage all depend heavily on operating conditions. Thus it can be concluded that:

(1) The minimum effective internal resistance of the Guppy cell is 40 micro-ohms. The resistance is nearly constant for currents of short-circuit magnitude for all battery conditions except the lower third of the discharge cycle where the resistance increases. The resistance varies from 40 micro-ohms to 80 micro-ohms for currents in the normal operating range (depending on the actual load and battery condition) and for short-circuit conditions in the lower third of the discharge. The minimum value of resistance can nevertheless be used for all fault calculations without introducing more than 5 percent error, except for the lower third of the discharge cycle.

(2) The overvoltage which exists during charging is capable of supplying current and hence should be used in maximum fault calculations.

(3) The maximum test currents attained were 47,000 amperes under normal battery conditions and 49,000 amperes with the battery at 85° F. The calculated maximum currents for zero fault resistance were 56,000 amperes and 60,000 amperes, respectively, for the above two battery states.

3707

(4) The recovery voltage is an inverse function of the transient load (ampere-seconds). A short circuit of 45,000 amperes for two cycles (0.033 sec) on the Guppy cell while on finishing rate will decrease the internal voltage from 2.57 to 2.25 volts. The maximum recovery voltage for all tests was 2.3 volts per cell.

RECOMMENDATIONS

It is recommended that the following values be used in design and analysis for systems employing Guppy batteries (Type MAQ-71):

(a) Effective internal resistance—40 micro-ohms per cell for any value of load applied during a charging or discharging cycle;

(b) Maximum recovery voltage—2.3 volts per cell.

It is further recommended that, where data is desired on the minimum internal resistance to be expected from a lead-acid cell, the value be obtained by short circuiting the cell just before it goes on the TVG curve.

ACKNOWLEDGMENTS

Acknowledgment is made of the ideas and material assistance rendered by Dr. J. C. White and E. E. Nelson of this laboratory, toward the prosecution of the experimental work. Their explanations of the chemical phenomena involved in the results have been most helpful.

* * *

APPENDIX I

Experimental Results on the Guppy Cell (Type MAQ-71)

Three Guppy cells were employed in the laboratory tests. All three were new, having been conditioned in accordance with the instructions supplied with the battery and cycled twice before testing was begun. The maximum charging current available was 900 amperes, which lengthened the charging cycle but should not otherwise affect the test results.

The complete plot of data for the four charging cycle tests is presented in Figures 17, 18, 19, and 20. Results of the discharge runs are shown in Figures 21 and 22. The variation in the load current curve for each test resulted primarily from the variation in battery internal voltage and secondarily from a small variation in the load resistance, the latter being due to temperature effects and contactor resistance.

The value of cell internal resistance was calculated from the test data using the following relationship:

$$E = V_d + I_l R,$$

where E = Battery internal voltage

V_d = Battery terminal voltage during loading (at 0.05 sec)

I_l = Battery load current (at 0.05 sec)

R = Battery internal resistance (effective value reflecting all changes taking place in the cell).

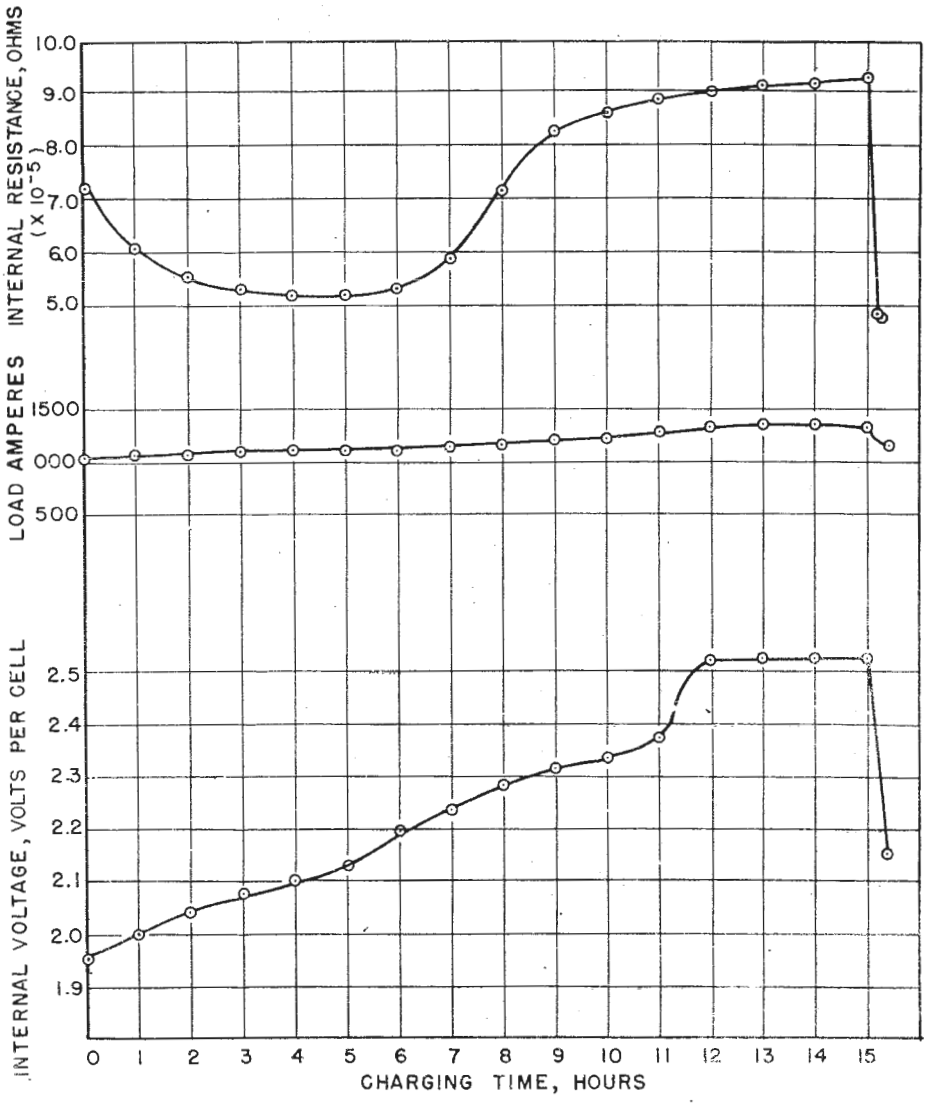

Figure 17 - Characteristics of Guppy cell (MAQ-71) at nominal 1000-ampere load during the charging cycle. Loading for 1.0 second every 20 minutes throughout the charging cycle and while floating. Charging source removed from the line 0.2 second before load imposed.

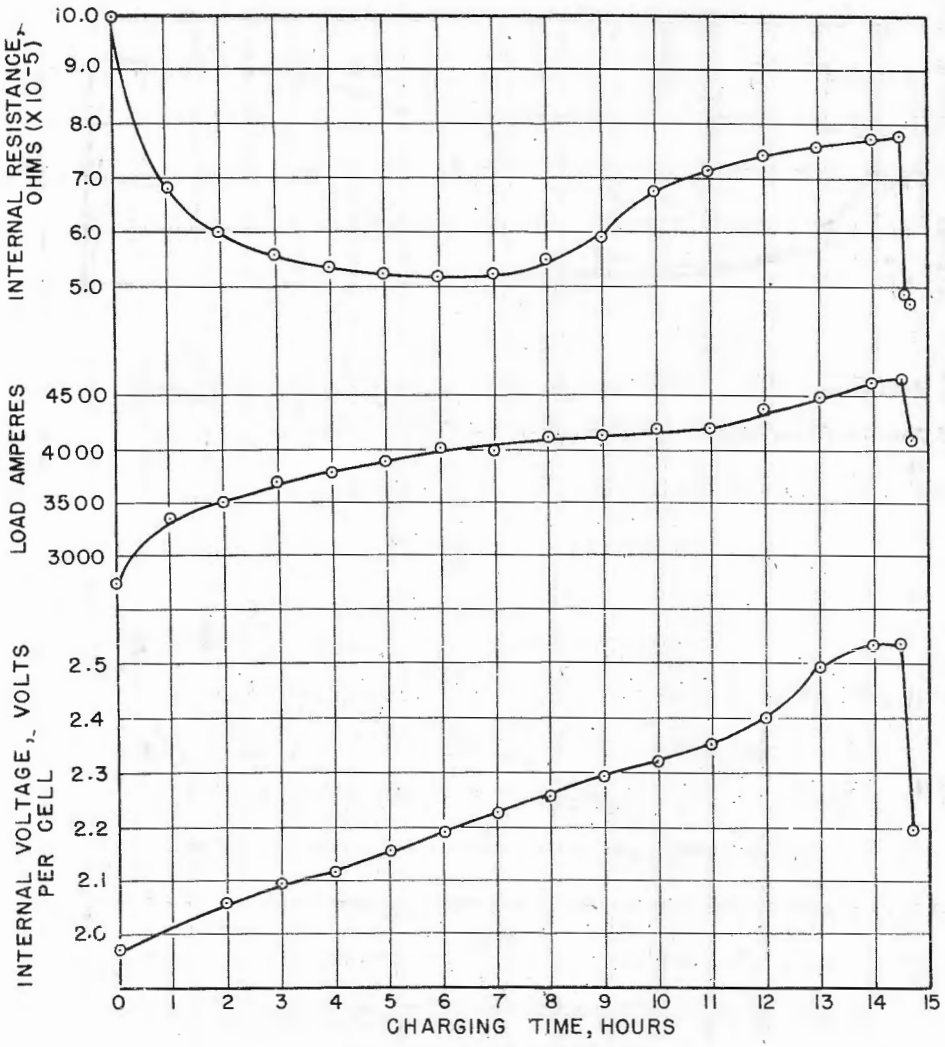

Figure 18 - Characteristics of Guppy cell (MAQ-71) at nominal 4000-ampere load during the charging cycle. Loading for 1.0 second every 20 minutes throughout the charging cycle and while floating. Charging source removed from the line 0.2 second before load imposed.

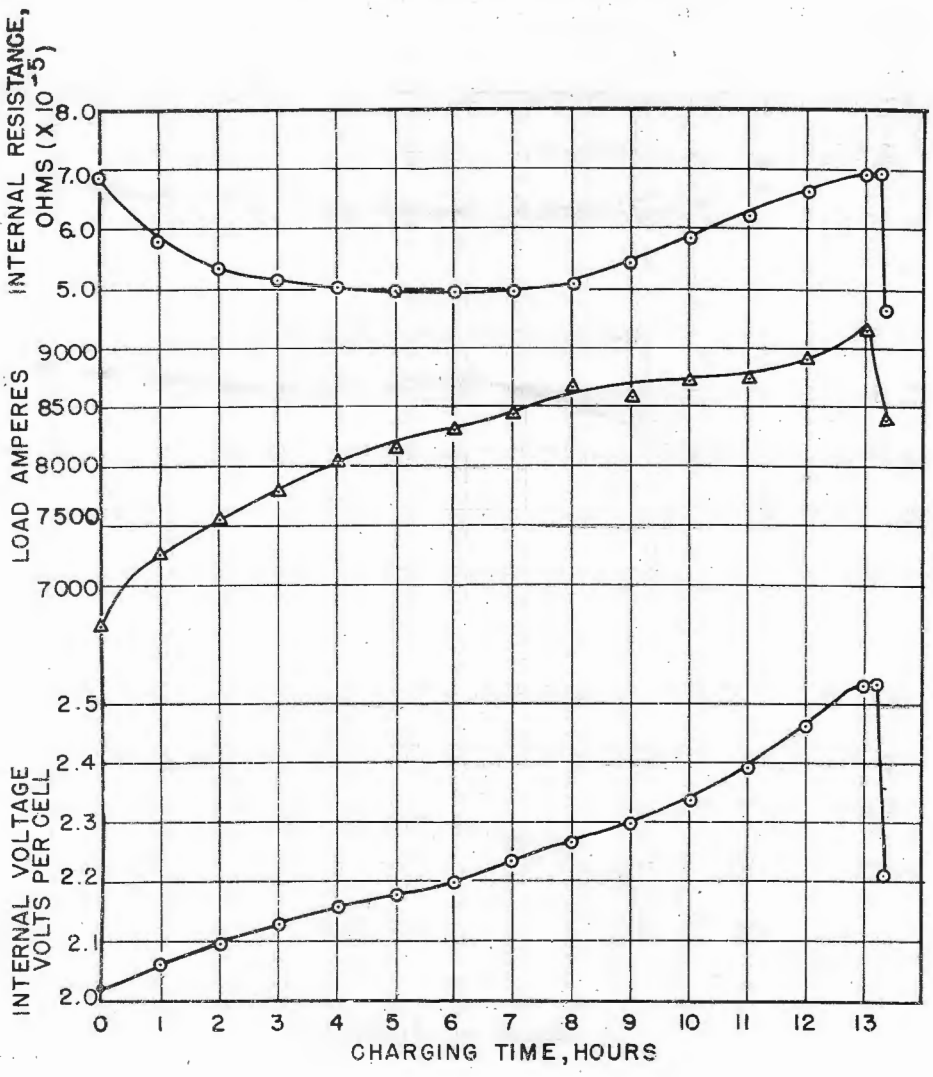

Figure 19 - Characteristics of Guppy cell (MAQ-71) at nominal 8000-ampere load during the charging cycle. Loading for 1.0 second every 20 minutes throughout the charging cycle and while floating. Charging source removed from the line 0.2 second before load imposed.

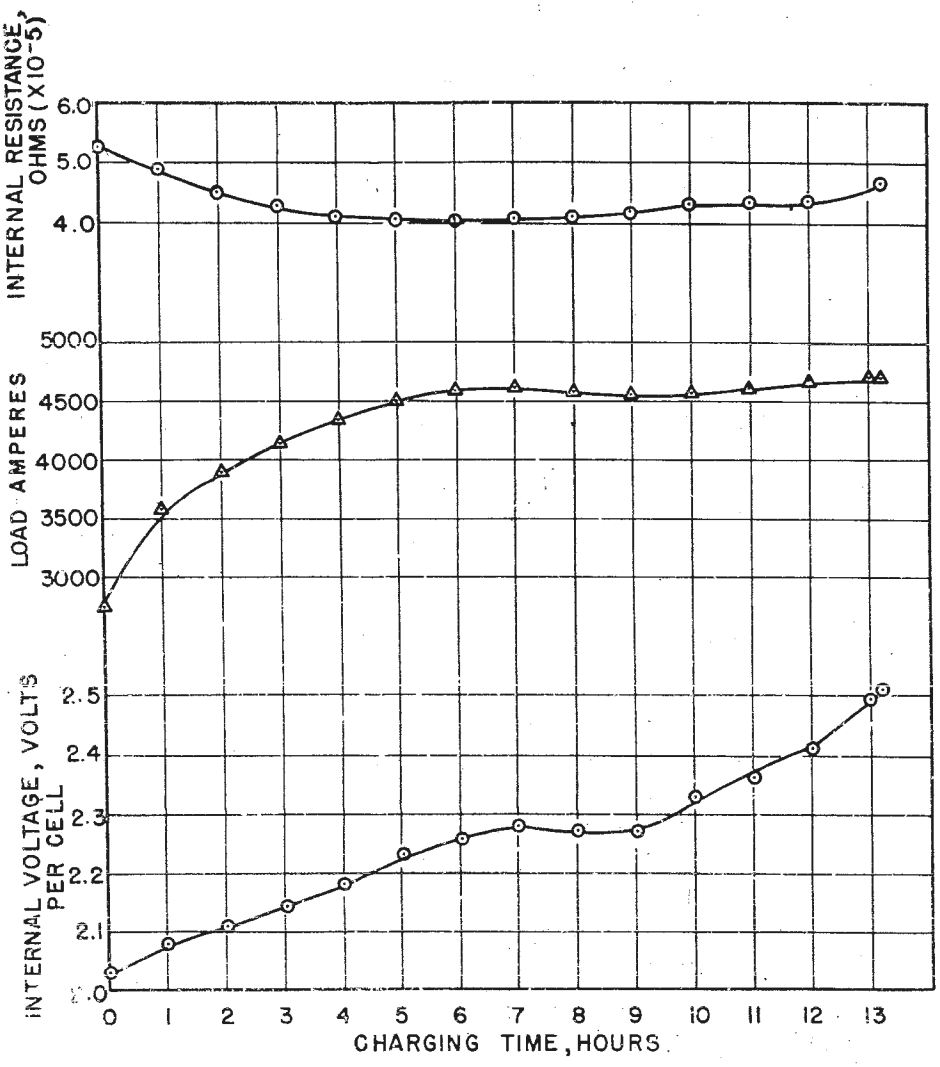

Figure 20 - Characteristics of Guppy cell (MAQ-71) at nominal 45,000-ampere load during the charging cycle. Loading for 1.0 second every 40 minutes throughout the charging cycle. Charging source removed from the line 0.2 second before load imposed.

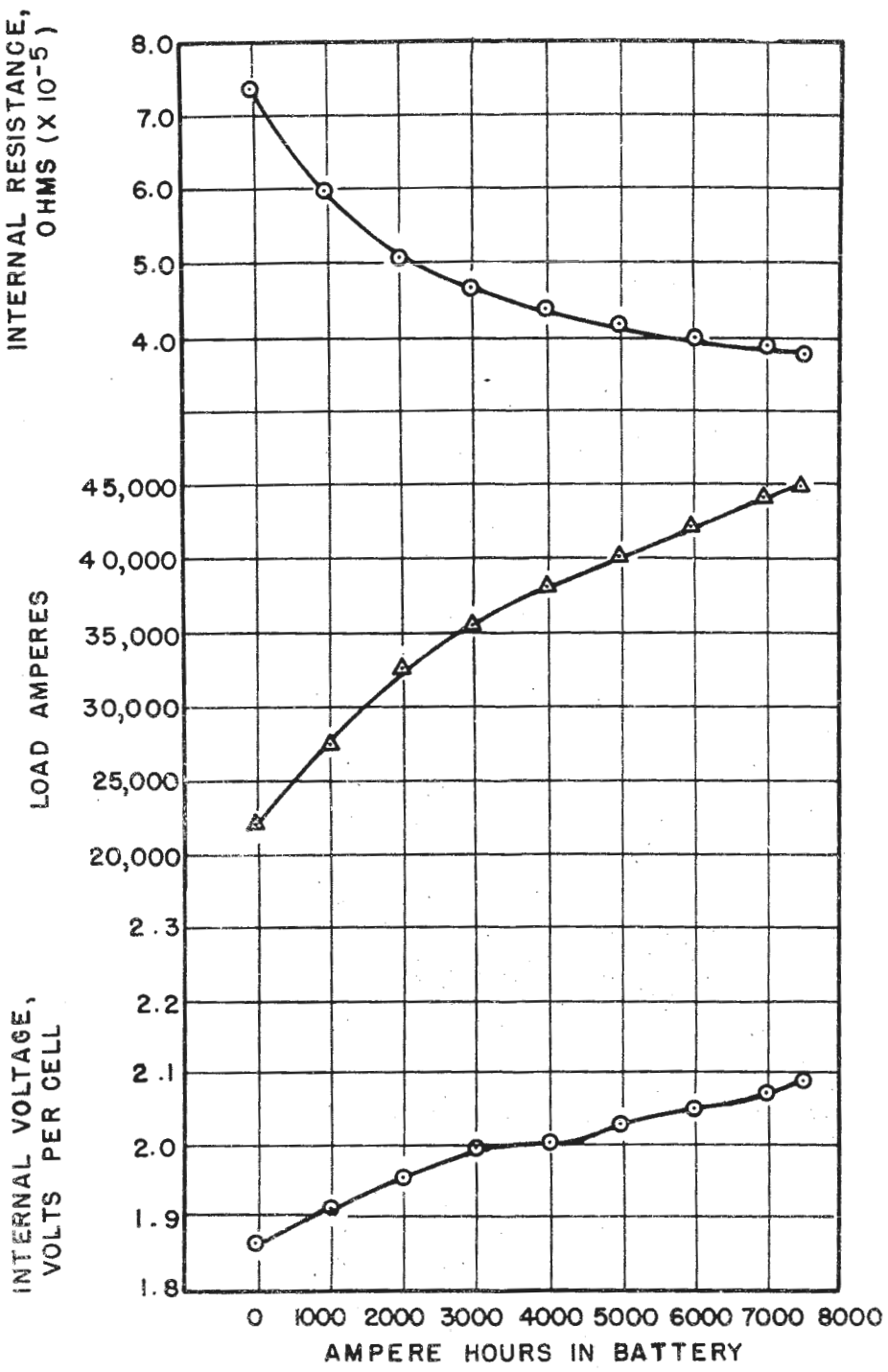

Figure 21 - Characteristics of Guppy cell (MAQ-71) at nominal 45,000-ampere load during the discharge cycle. Loading for 1.0 second every hour throughout the discharge cycle. Discharge load (1000 amperes) removed from line 0.2 second before load imposed.

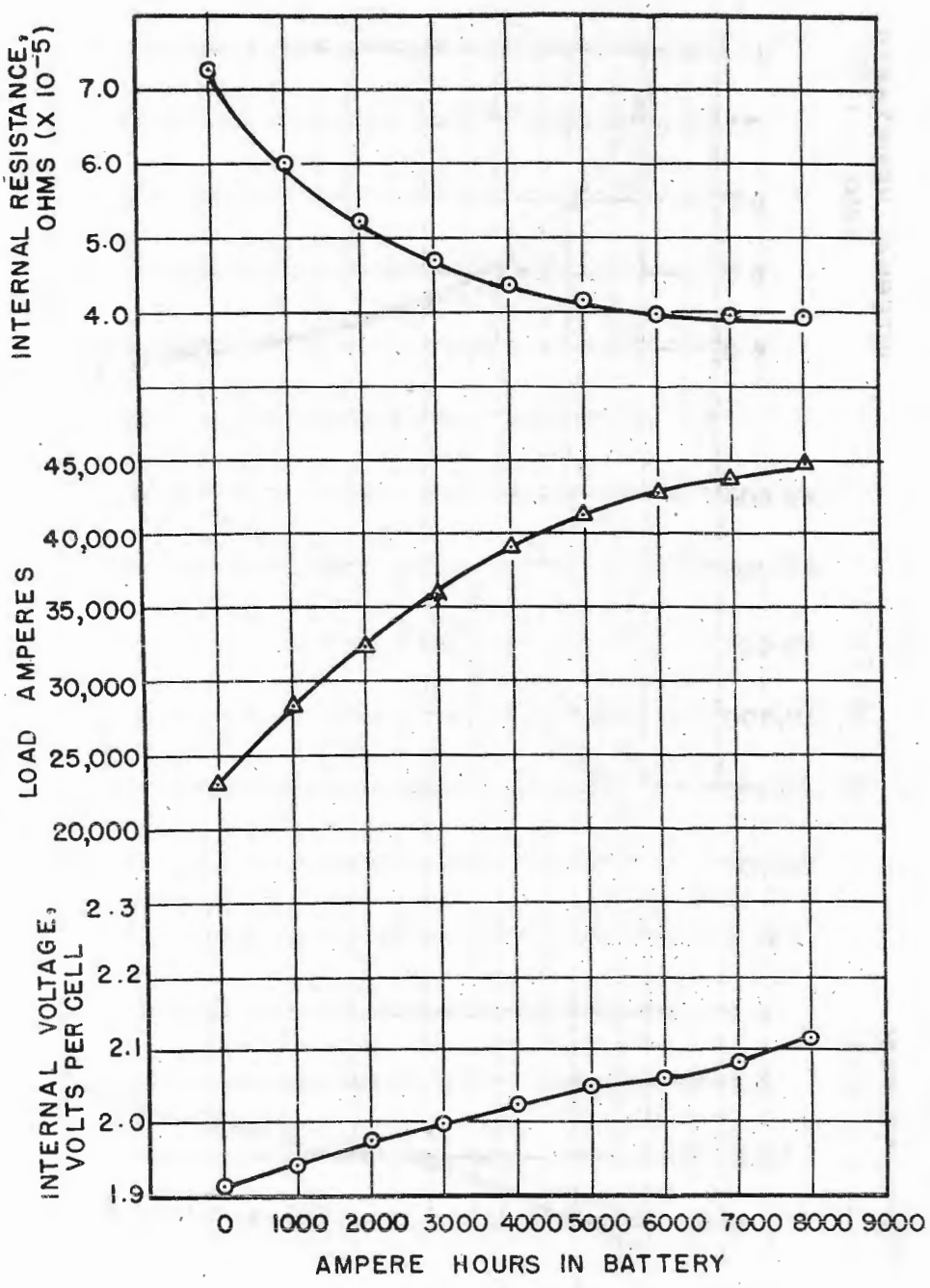

Figure 22 - Characteristics of Guppy cell (MAQ-71) at nominal 45,000-ampere load during the discharge cycle. Discharge at the 1000-ampere rate for one hour, rest unloaded for one hour, then loading for 1.0 second.

APPENDIX II

Experimental Results on the Sargo Cell (Type VLA-47)

Studies on the Sargo cells were made on the 126-cell submarine battery at the Submarine Base, New London, Connecticut. A General Electric 415-volt, 2650-ampere, 750-rpm generator was used in conjunction with the battery.

The battery was prepared for the tests by giving it a full charge and then discharging it 6000 ampere-hours at a 2500-ampere rate. The next day another 400 ampere-hours were taken out of the battery before testing. The battery was then put on charge and the tests carried out during the course of the charging cycle. The plots of the battery terminal voltage and charging current are presented in Figure 23, but the lines joining the points are merely for convenience in following the trend and do not represent the actual way in which these quantities varied. The charging current was actually maintained at the test value for 5 to 15 minutes before the test.

Calculations of the battery internal voltage and internal resistance were carried out using

$$E = V_b - I_c R$$

$$E = V_d + I_l R,$$

where E = Battery internal voltage

V_b = Battery terminal voltage before loading (while charging)

V_d = Battery terminal voltage during loading (at 0.12 sec)

I_c = Battery charging current

I_l = Battery load current (at 0.12 sec)

R = Battery internal resistance (effective value reflecting all changes taking place in the cell).

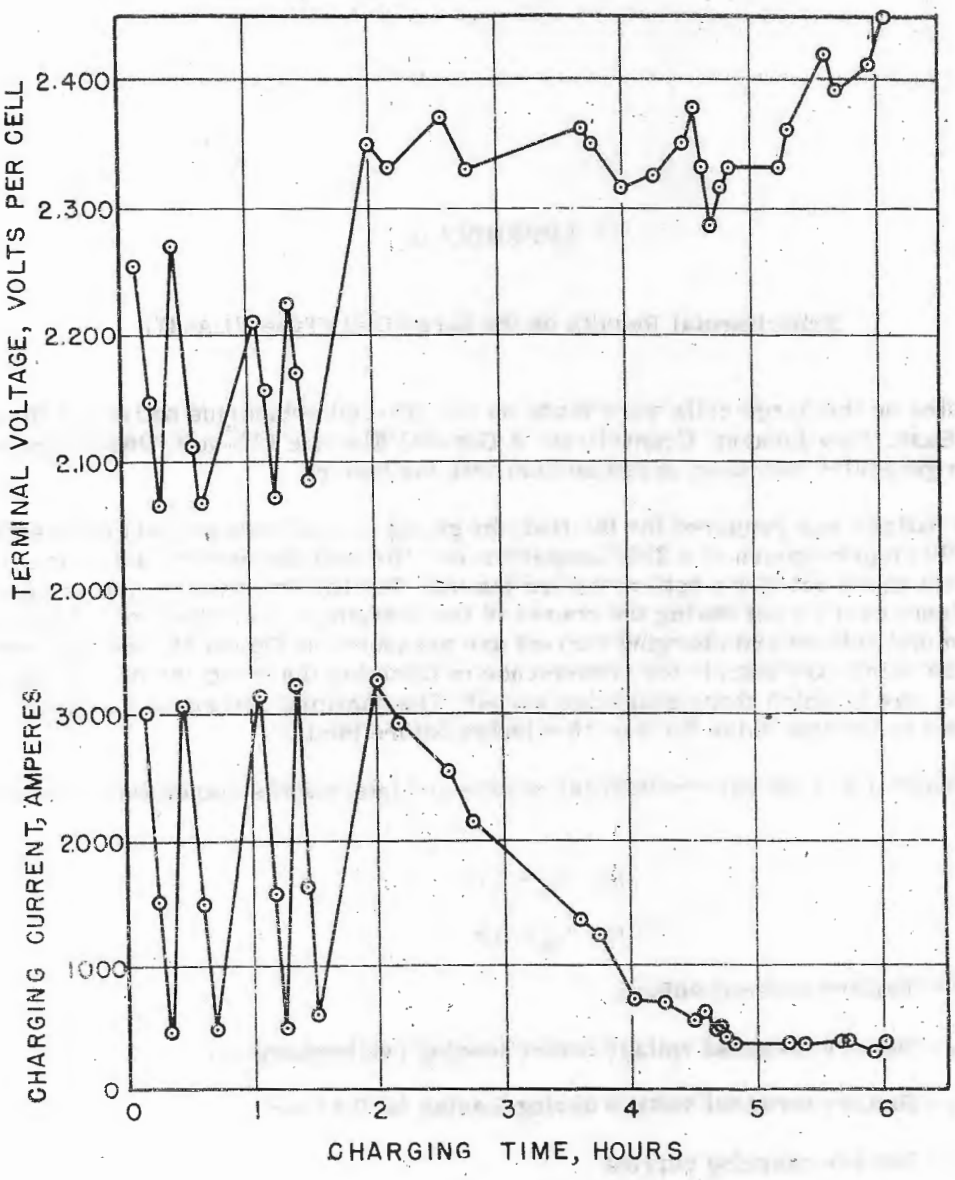

Figure 23 - Terminal voltage and charging current of the Sargo cell (VLA-47) during the charging cycle

* * *